



Experimental studies of Bose–Einstein condensates in disorder

Yong P. Chen ^{*,1}, J. Hitchcock, D. Dries, M. Junker, C. Welford, S.E. Pollack, T.A. Corcovilos, R.G. Hulet

Department of Physics and Astronomy and Rice Quantum Institute, Rice University, 6100 Main Street, Houston TX 77005, USA

ARTICLE INFO

Article history:

Available online 11 February 2009

PACS:

03.75.Hh

03.75.Kk

64.70.Tg

Keywords:

Matter wave

Bose–Einstein condensate

Interaction

Disorder

Superfluid

ABSTRACT

We review recent studies of the effects of disorder on an atomic Bose–Einstein condensate (BEC). We focus particularly on our own experiments with ⁷Li BECs in laser speckle. Both the interaction, which gives rise to the nonlinearity in a BEC, and the disorder can be tuned experimentally. This opens many opportunities to study the interplay of interaction and disorder in both condensed matter physics and nonlinear science.

© 2009 Elsevier B.V. All rights reserved.

1. Introduction

Since their experimental realizations in 1995, Bose–Einstein condensates (BEC) of ultracold atoms [1,2] have had significant impact on several branches of modern physics. For example, the intrinsic cleanliness coupled with remarkable controllability of physical parameters have made cold atom systems an exceptional venue to study a rich variety of problems in condensed matter physics, ranging from superfluidity to strongly-correlated systems. In particular, cold atoms in optical lattices (*periodic* potentials) could become a powerful “quantum emulator” for many-body physics (see reviews in [3–5]).

As a coherent matter wave, a BEC also provides an extremely interesting system to study in nonlinear science [6]. On a mean-field level, a BEC is described by the well-known Gross–Pitaevskii equation (GPE), the time-dependent version of which reads:

$$i\hbar \frac{\partial \Psi(\vec{r})}{\partial t} = \left(-\frac{\hbar^2}{2m} \nabla^2 + V(\vec{r}) + g|\Psi(\vec{r})|^2 \right) \Psi(\vec{r}), \quad (1)$$

where $\Psi(\vec{r})$ is the condensate wavefunction, m is the atomic mass, $V(\vec{r})$ is the external potential (for example, the trap potential that confines the atoms) and $g = 4\pi \hbar^2 a_s/m$ with a_s being the s -wave scattering length [1]. The GPE is a *nonlinear* Schrödinger

equation [7], with analogous forms appearing in nonlinear optics and many other nonlinear systems. We emphasize that for the BEC, it is the (mean-field) interaction $U = gn$, where $n = |\Psi(\vec{r})|^2$ is the atomic density, that gives rise to the nonlinear term in (1). Such nonlinearity gives rise to many interesting phenomena in BECs [6], among the most remarkable examples being the observations of various forms of matter wave solitons [8–11].

BECs subjected to disorder (i.e., random potentials) [12] have received great attention in the past few years. Disorder plays a fundamental role in modern condensed matter physics as most real materials inevitably contain defects, which are often difficult to control. The intrinsic cleanliness of cold atom systems, with the ability to introduce well-controlled disorder, offers unique opportunities to study disordered quantum systems [13,14] and uncover novel quantum phases [5,15]. Studying disordered BECs may also provide valuable insight to understand the behavior of nonlinear systems in the presence of randomness. Since 2005, there has been a flurry of experimental activities [16–27] to study BECs in disordered potentials. The physics investigated has included disorder induced inhibition of transport [16–19,21], effects of disorder on collective modes [16,21,24], Bose glass [20], granular BEC and phase coherence [21], density modulations [21,22], disordered Bose–Hubbard model [23], Anderson localization [25,26] and solitons in disorder [27].

In this article, we review our recent experiments [21,27] on a ⁷Li BEC with *tunable* interactions and subject to a well-controlled disorder made by laser speckle. In the regime of strong repulsive interactions, we have observed that increasing disorder turns the BEC from a superfluid (with expected phase coherence) into an insulating and fragmented “granular” condensate with no global

* Corresponding author.

E-mail address: yongchen@purdue.edu (Y.P. Chen).

¹ Current address: Department of Physics, Purdue University, 525 Northwestern Ave., West Lafayette, IN 47904, USA.

phase coherence. In the regime of moderate attractive interactions, we have performed preliminary studies on the behavior of matter wave solitons in disorder. Our experiments enable studying the interplay between disorder and interaction (or nonlinearity), a topic of great interest in condensed matter and nonlinear physics.

The rest of the paper is organized as follows. In Sections 2 and 3 we review the experimental methods to realize tunable interactions and tunable disorder respectively. These technologies are key for studying the physics discussed in this paper. In Section 4, we review the experiments on disordered BECs under various physical conditions, focusing on our results on *interacting* BECs. The article is concluded in Section 5.

2. Tunable interactions

From Eq. (1) we see that the mean field interaction $U = gn = 4\pi\hbar^2 na_s/m$ can be controlled by controlling the atom density (n) or the scattering length a_s . The first method (controlling n) was used, for example in [25] to reduce the strength of (repulsive) interaction to be sufficiently weak to realize Anderson localization [13]. The second method (controlling a_s , for example, via a magnetic Feshbach resonance [28] that tunes a_s by an external magnetic field (B)) is more versatile because both the strength as well as the sign of the interaction can be tuned (from repulsive to attractive). One could in principle reduce the interactions to much smaller strength than what may be practically possible with reducing n (without sacrificing the measurement signal at low n). Several recent experiments [26,27], including ours, have used a Feshbach resonance to tune the interactions.

In our case [21,27], we use the magnetic Feshbach resonance, located near 737 G, in the ($F = 1, m_F = 1$) state of ^7Li [9,10,29,30]. This resonance (Fig. 1) is broad, extending several hundreds of Gauss and alleviating the stringent experimental requirements on controlling and stabilizing the magnetic field. A particularly appealing feature of this broad resonance is the existence of an extremely gradual zero-crossing in the B dependence of a_s [9,10,27,30]. Using this Feshbach resonance, we can tune the interactions in a wide range to access markedly different regimes, including:

- *strongly repulsive*, where the BEC wavefunction (in the absence of disorder) is well described by the Thomas–Fermi approximation [1] of the GPE (1);
- *(nearly) non-interacting*, where the BEC wavefunction is well described by the *linear* Schrödinger equation;
- *moderately attractive*: where the BEC can form into one or several bright matter wave solitons [9,10]. The solitons are stabilized by a quasi-1D trap geometry we use in our experiments.

The remarkable control of the interactions in ^7Li is demonstrated in Fig. 1.

3. Tunable disorder

Recent experiments on disordered BECs have mostly used various forms of *optically generated* disorder. In contrast to the disorder due to material defects in typical solid state systems, such optical disorder is of great advantage because the disordered potential is easily tunable and can be precisely characterized. Three types of optical disorder have been used so far: laser speckle [16,18,21], image of a disordered substrate [19,24] and quasi-random (incommensurate) optical lattices [20,26]. The different types of disorder could lead to different physics of disordered BECs, as has been discussed in the case of disorder-induced localization [12]. Laser speckle [31], which we use in our experiments, has been the simplest and most popular method to generate optical disorder.

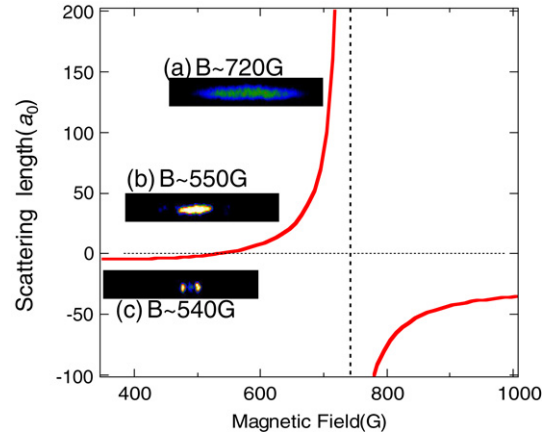


Fig. 1. Calculated scattering length a_s (in units of Bohr radius a_0) as a function of magnetic field B for ^7Li (in the state derived from the ($F = 1, m_F = 1$) Zeeman level, which we use in our experiment). The slope of a_s vs. B at the zero-crossing is $\sim 0.1 a_0/\text{G}$ [30]. Insets (b)–(c) demonstrate the effect of changing B (thus the interaction) on the BEC: (b) ~ 720 G (strongly repulsive); (c) ~ 550 G (weakly repulsive); (d) ~ 540 G (weakly attractive, where solitons are formed [9,10]). The color scale is individually defined for each inset for clarity.

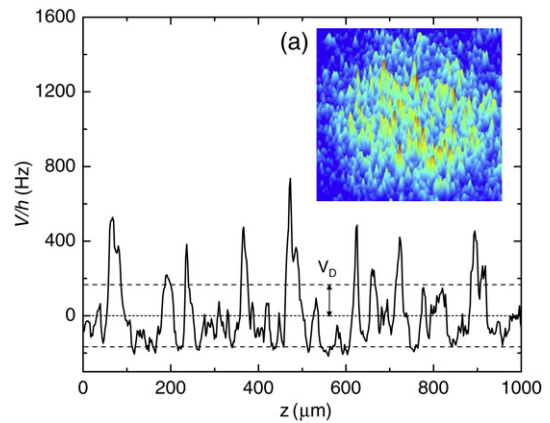


Fig. 2. Typical 1D disordered potential $V(z)$ (adapted from [21]). $V(z)$ is an axial cut $V(0, 0, z)$ of the 3D disordered potential $V(x, y, z)$ through the center ($x = y = 0$) of the atomic cloud. Inset: False-color surface plot of the 2D cross-section $V(0, y, z)$ of the disordered speckle potential as imaged by a camera. The pixel size corresponds to $2.2 \mu\text{m}$ in the plane of the atoms.

The procedure to create laser speckle in our experiments has been described in detail in [21] and is similar to that used in [16,18]. In our case, the BEC, with its small radial size compared to the length scale of the speckle, is to a good approximation subject to a 1D disordered potential $V(z)$. A representative disordered potential is shown in Fig. 2. The disorder strength, V_D , proportional to the intensity of the speckle laser, is defined as the standard deviation about the mean of $V(z)$. The disorder correlation length [18,21,31], σ_z , is related to the diffraction limit of the optical system used to generate the speckle [18,31].

4. Experiments on disordered BECs

In this section we review our experiments on *interacting* ^7Li BECs in disorder, focusing on the physics of the interplay between disorder and nonlinearity. A comprehensive review covering many other experiments on disordered BECs can be found in [12]. Discussions on the rich physics related to BECs subject to both disorder and *optical lattices*, not covered in this article, can be found in [5,20,23].

4.1. Repulsive interaction regime

We recently reported a systematic study [21] of a repulsively interacting ^7Li BEC in a disordered potential, whose strength (V_D) can be tuned from zero to above the BEC chemical potential (μ). We have studied both the transport properties and phase coherence of the disordered BEC. We review the experimental observations in this subsection and discuss their physical implications.

4.1.1. Experimental parameters

The procedure we use to create a large repulsive ^7Li BEC has been described in detail in [21] and is similar to that used in [10,29]. Except where otherwise specified, the typical parameters of the BEC in our experiments [21] are: scattering length $a_s \sim 200a_0$, number of atoms $N \sim 5 \times 10^5$, radial trap frequencies $\omega_x = \omega_y \simeq 2\pi \times 180$ Hz, and the axial trap frequency $\omega_z \simeq 2\pi \times 3.6$ Hz. For such a BEC, the chemical potential $\mu \approx h \times 1$ kHz, where h is Planck's constant. After producing the BEC, the speckle disordered potential ($\sigma_z \sim 15 \mu\text{m}$) is ramped on to a specific value of V_D . The BEC is then held in the disordered and trap potentials while various experiments are performed. The final state is probed by absorption imaging of the atomic cloud released from the disordered and optical trap potentials, or by *in situ* polarization phase contrast imaging [32]. Both the imaging and speckle lasers propagate along the x -axis.

4.1.2. Transport properties

To characterize the transport properties of the disordered BEC, we have carried out two different types of measurements, which we refer to as “dipole oscillation” and “slow drag”, with the results summarized in Fig. 3.

In the “dipole oscillation” experiment (Fig. 3a–b), the center of the harmonic trap is *abruptly* offset, and the cloud evolves in the presence of the shifted trap and stationary disorder for a variable time before being released for absorption imaging. Without disorder, the condensate undergoes undamped dipole oscillations in the trap with frequency ω_z . These oscillations are damped at finite disorder (even as small as $V_D \sim 0.1 \mu$) and overdamped for $V_D \gtrsim 0.4 \mu$. The damping coefficient β was found to relate to V_D by a power law, $\beta \propto (V_D/\mu)^{5/2}$ [27,33]. When $V_D \gtrsim \mu$, the cloud becomes pinned at its initial position to within our experimental resolution.

In the “slow drag” experiment, we *slowly* (in $\sim 1\text{s}$) ramp on a magnetic field gradient along the z direction, which offsets the center of the harmonic trap from $z = 0$ to $z = -d$. The disordered potential is kept stationary during the trap offset. The cloud center as a function of V_D for 4 different offset distances d is plotted in Fig. 3c. Without disorder, the center of the atomic cloud follows the trap. For intermediate disorder strength, we have found that the cloud lags behind the new trap center and is stretched [21], indicating inhibited transport. For stronger disorder ($V_D \gtrsim 0.8 \mu$), the cloud is pinned at its initial position and does not respond to the offset.

4.1.3. Time of flight (TOF) measurements and phase coherence

We have performed both *in situ* (phase contrast) and TOF (absorption) imaging on the disordered BEC, yielding information on both its density and phase. Phase contrast imaging [32] is important to obtain accurate *in situ* density profiles of the atoms due to the high optical density of the trapped BEC.

Fig. 4 compares the *in situ* images (a1–a4) and corresponding TOF (taken 8 ms after releasing the cloud) images (c1–c4) for various V_D (from top to bottom, $V_D/\mu \approx 0, 0.3, 0.5$ and 1.0 , respectively). The corresponding axial cuts (column densities), (b1–b4) for *in situ* and (d1–d4) for TOF, are also shown. For intermediate V_D , striking random fringes, which we interpret

as matter wave interference, develop after sufficiently long TOF expansion of the BEC following release from the optical potentials (for example, Fig. 4 (c3, d3), where $V_D/\mu \sim 0.5$). We note that at such V_D , the corresponding *in situ* images (Fig. 4 (a3, b3)) are consistent with the cloud still being *connected*. By increasing V_D above μ , the disordered BEC becomes *fragmented*, as shown in the *in situ* profile (Fig. 4 (a4, b4)), and the fringe contrast observed in TOF diminishes, as shown in Fig. 4 (c4,d4). Detailed analysis [21] shows that the TOF fringe contrast peaks at $V_D \simeq 0.5 \mu$, while the contrast in the *in situ* images increases up to the highest V_D investigated.

4.1.4. Discussion

TOF interference fringes probe the phase coherence in the trapped disordered BEC. Similar, but less well resolved fringes in TOF images have been reported previously [16,19]. Our highly elongated BEC facilitates a systematic and quantitative study of the fringes. We find the positions of these irregularly spaced fringes are *reproducible* in repeated measurements, even with different holding times of the BEC in the disordered potential. Another recent experiment [22] has reported reproducible fringes in TOF images of a disordered ^{87}Rb BEC. The reproducibility suggests that these fringes are unlikely due to some initial (before release) phase fluctuations [34] in the disordered BEC, or due to interference of a few BECs separated by high potential barriers with no well defined relative phase between them, as in either of these scenarios the fringe positions are not expected to be reproducible. We interpret the reproducible and spatially random density fluctuation we observe in the long time of flight images at intermediate disorder strength as due to the matter wave interference from different parts of the disordered, yet phase coherent, BEC after it is released. This is conceptually analogous to laser speckle, which is the random intensity fluctuation produced by interference from different parts of a phase coherent light (laser) re-scattered from a rough surface. In both cases, phase coherence is crucial for the reproducibility of the resultant density or intensity fluctuation pattern.

Numerical simulations based on the Gross–Pitaevskii equation [19,22] have shown that such interference can occur when moderate disorder-induced density fluctuations cause different parts of a *phase coherent* BEC to expand with different velocities and overlap. As V_D is increased from 0, the contrast of the interference is expected to increase at small V_D . When V_D becomes sufficiently large, however, the BEC fragments into multiple pieces, as is seen in the *in situ* image, Fig. 4 (a4,b4). An array of *randomly spaced* condensates should not produce visible interference in TOF [35,36], again consistent with our observation of diminishing fringe contrast at high V_D (Fig. 4 (c4,d4)). This is quite different from the case of an array of *periodically* spaced condensates (with negligible tunneling between them), which can still give rise to finite interference (but not reproducible) in a one-shot measurement [35,36].

Regarding the transport properties, we observe completely inhibited transport (pinning of the condensate) at high V_D , indicating a transition to an insulator. This was seen in previous transport experiments, where the nature of the insulator is inferred to be that of a fragmented BEC [16–18]. Our *in situ* images give the first direct observation of fragmentation of a highly disordered BEC. Because of the exponentially suppressed Josephson tunneling between fragments due to high potential barriers, the fragmented BEC is expected to have large phase fluctuations and no phase coherence [37]. This regime is analogous to a granular superconductor [38,39], which is an insulator without global phase coherence.

Dipole oscillations are damped at moderate V_D , as shown in Fig. 3(a, b), and in agreement with previous observations [16]. Excitations such as solitons, vortices, and phase slips have been

Fig. 3. Effect of disorder on the dipole oscillations (a, b) and slow transport (c) of BEC. See text for details. Figure adapted from [21].

Fig. 4. *In situ* profiles and TOF matter wave interference of disordered BEC. (a1–a4) *In situ* images for $V_D/\mu \approx 0, 0.3, 0.5$ and 1.0 , respectively; (b1–b4) *In situ* column-density profiles (axial cuts for images a1–a4); (c1–c4) TOF images taken 8 ms after releasing the BEC, for $V_D/\mu \approx 0, 0.3, 0.5$ and 1.0 , respectively; (d1–d4) TOF column-density profiles (axial cuts for images c1–c4). Solid red lines are fits to Thomas–Fermi distributions. $\omega_z \simeq 2\pi \times 2.8$ Hz for data shown here. The TOF 2D image uses a different color scale from the one used for the *in situ* 2D image, and the displayed aspect ratio of the *in situ* images is reduced by 50% in order to enhance the transverse size for visibility. Part of figure adapted from [21]. (For interpretation of the references to colour in this figure legend, the reader is referred to the web version of this article.)

suggested [40] as possible mechanisms giving rise to damping. This is consistent with Landau’s criterion for the destruction of superfluidity [1], as we note that at small V_D , the sound velocity of the BEC at the center of the cloud $c = \sqrt{\mu/m} \sim 8$ mm/s, which is comparable or even smaller than the maximum speed of the moving BEC relative to the static disordered potential (Fig. 3 (a, b)). Our *in situ* as well as TOF data at moderate V_D suggest a disordered BEC that is still connected (not yet fragmented) and phase coherent, in order to give a reproducible interference pattern. Rather than being “granular”, this regime is analogous to

a “homogeneous” disordered superconductor [38]. Damped dipole oscillations were also recently studied for a BEC in a periodic potential [41] in the context of a possible “Bose metal” phase [42].

Disordered superconductors (either “granular” or “homogeneous” thin films) have been studied extensively [38] in condensed matter physics, in the context of a disorder induced superfluid/superconductor to insulator transition (SIT), and so-called “dirty boson” problem [14], which is also relevant for superfluid helium in porous media [43] and random Josephson junction arrays [44]. While many believe that such a SIT is a quantum phase

